

Molecular motion of DNA as measured by triplet anisotropy decay

(flexible rod/local motion)

M. HOGAN*, J. WANG*, R. H. AUSTIN†, C. L. MONITTO†, AND S. HERSHKOWITZ†

*The Departments of Biochemical Sciences and †Physics, Princeton University, Princeton, New Jersey 08544

Communicated by John J. Hopfield, February 16, 1982

ABSTRACT We have used triplet anisotropy decay techniques to measure the internal flexibility and overall rotational motion of DNA, covering a time range from 15 ns to 200 μ s. Nearly monodisperse DNA fragments 65–600 base pairs long were studied by using the intercalating dye methylene blue as a triplet probe. We found that the slow end-over-end tumbling of short DNA fragments (≤ 165 base pairs) is as predicted for a rigid rod. As expected, a longer DNA fragment (600 base pairs) experiences slow segmental motion of its helix axis. We found that, at the earliest times, anisotropy decays more rapidly than expected for a rigid rod, suggesting that, when bound, methylene blue monitors fast internal motion of the helix. Since the rod-like end-over-end tumbling of short fragments rules out fast bending motions, we conclude that the fast components of DNA anisotropy decay are due to twisting motion of the helix, occurring with a time constant near 50 ns.

Under physiological conditions, B-form DNA is an exceedingly stable structure. Recently, however, evidence has accumulated suggesting that the structure of the helix fluctuates substantially (1–8). It has been shown by NMR techniques (1–4) that the helix experiences large fast motions in the nanosecond time range. Fast motions in the 1- to 100-ns time range have also been seen by fluorescence anisotropy methods (5–7), using as a probe ethidium bromide intercalated in DNA, and by measuring the ESR line shapes of spin-labeled intercalated dyes (8).

Here we describe triplet anisotropy decay measurements of DNA internal motions. As in fluorescence anisotropy measurements, we have used an intercalating dye as a probe; however, we have monitored the anisotropy decay of the triplet rather than the singlet state by using methylene blue, a dye with a high triplet yield. Since the triplet lifetime of methylene blue is $\approx 100 \mu$ s, we can use triplet anisotropy decay techniques to measure motions over a time scale 1,000 times larger than fluorescence methods allow.

MATERIALS AND METHODS

In time-resolved triplet anisotropy measurements, chromophores bound rigidly to macromolecules are excited by a short pulse of linearly polarized light. For dyes with high triplet yields, a population of oriented triplet-state molecules results, oriented here meaning that the angular distribution of excited dipole moments is not spherically isotropic. Via rotational Brownian motion, the angular distribution will randomize in time, and the time dependence of the return to a spherically isotropic distribution of dipoles can be monitored either by observing the polarization of the triplet-singlet emission (phosphorescence) or by measuring the absorbance anisotropy associated with the triplet state.

In the triplet-state anisotropy decay experiments described

here, we have monitored the absorbance anisotropy of the depleted singlet state rather than the triplet state directly. The two techniques are interchangeable; however, singlet-state measurements are often more sensitive because of the higher absorption coefficient of the singlet manifold. Triplet-state absorption spectra are usually red shifted to the singlet spectra and usually have smaller absorption coefficients. By using a monitoring beam at the singlet transition frequency, it is possible to measure the decrease in absorbance that occurs when singlet chromophores undergo intersystem crossing to the triplet state.

The apparatus we have constructed to monitor triplet anisotropy decay is similar to that described in ref. 9. Our excitation source was a rhodamine 640 dye laser (λ_{ex} , 604 nm) pumped by a frequency-doubled Nd:YAG pulsed laser (Moletron MY-32). The laser was operated at 10 Hz with an average energy of 0.65 mJ per pulse and a pulse width of 15 ns (full width at half maximum intensity). The excitation pulse from the dye laser was vertically polarized by a polaroid filter. The monitoring beam was produced by a linearly polarized He/Ne laser (λ , 632.8 nm).

A microcomputer-driven rotating polarizer was used to observe the polarization of the monitoring beam both parallel and perpendicular to the excitation polarization. Data were stored on a Biomation 6500 transient recorder with a maximum sample rate of 2 ns per point. A microcomputer was used to control the transient recorder and to signal average.

The computer analyzed the two files stored to compute the time-resolved anisotropy decay

$$r(t) = \Delta I_{\parallel}(t) - \Delta I_{\perp}(t) / \Delta I_{\parallel}(t) + 2\Delta I_{\perp}(t) \quad [1]$$

and the isotropic absorbance decay

$$a(t) = \Delta I_{\parallel}(t) + 2\Delta I_{\perp}(t), \quad [2]$$

where $\Delta I_{\parallel}(t)$ and $\Delta I_{\perp}(t)$ refer to monitoring beam intensity changes for polarization parallel and perpendicular, respectively, to the excitation pulse polarization. Since typical transmission changes were 5% or less (20 mV out of 500 mV), intensity changes were directly proportional to changes in absorbance.

DNA fragments were prepared from calf thymus DNA (Sigma). DNA was dissolved in 0.1 M NaOAc/2 mM ZnSO₄, pH 4.6, and then digested for 20 min at 37°C with DNase I and nuclease S1 at 30 and 1,000 units, respectively, per mg of DNA. The reaction was quenched by adding Na₂EDTA to 10 mM. Nuclease S1 is in excess under these conditions to ensure that single-stranded DNA regions are eliminated. The resulting short DNA fragments were digested with heat-treated RNase A and then with bacterial protease and phenol extracted to remove protein fragments. All enzymes were purchased from Sigma.

DNA fragments were fractionated by length on a Sepharose 6B gel column (Pharmacia). The lengths of the DNA fragments

The publication costs of this article were defrayed in part by page charge payment. This article must therefore be hereby marked "advertisement" in accordance with 18 U. S. C. §1734 solely to indicate this fact.

Abbreviation: bp, base pair.

were estimated from their electrophoretic mobilities on 5% acrylamide gels relative to that of a *Hae* III restriction enzyme digest of ϕ X174 (obtained from New England BioLabs). Photographic negatives of ethidium bromide-stained gels were scanned with a Joyce-Loebl densitometer. Length distributions given in the text correspond to the length range that contained 80% of the total ethidium fluorescence intensity of the sample.

Integrity of the DNA samples is of importance in this work. For that reason, we assayed the DNA preparations by redigesting the samples analytically with nuclease S1, using the protocol described in ref. 2. Under these assay conditions, any single-stranded DNA is digested completely (2). In all cases, the fractionated DNA samples used for anisotropy measurements contained 1% or less of material that could be digested with nuclease S1. After heat denaturing the samples in 80% formamide, the nuclease S1-digested samples and undigested samples were subjected to electrophoresis on denaturing 0.05 M NaOH/2% agarose gels. In all cases, the (now single-stranded) nuclease S1-digested material and undigested material had identical mobilities relative to those of the DNA markers. Based on these assays, we are confident that the DNA used in this work is free from internal nicks or single-stranded regions.

Methylene blue was purchased from Eastman and was purified by column chromatography on an LH20 gel (Pharmacia), eluting with methanol. The resulting dye was assayed as pure by TLC [silica gel; chloroform/methanol/acetic acid (8:1:1)]. Samples were prepared for anisotropy measurements by adding concentrated solutions of methylene blue directly to DNA solutions. The standard buffer in all anisotropy measurements was 50 mM NaCl/5 mM Tris·HCl/1 mM EDTA, pH 7.5. Measurements were made at 5°C in a thermostatted cuvette. The standard methylene blue concentration was 5 μ M and the standard DNA concentration (in base pairs) was 0.5 mM. A two-fold variation in the DNA concentration or in the DNA/dye ratio did not have any effect on the time evolution of the decay curves (data not shown).

Anisotropy, as defined by Eq. 1, can be used to determine molecular motions. For a spherical molecule, the anisotropy decays as a single exponential, with a time constant that is a direct measure of its rotational diffusion coefficient D :

$$r(t) = r(0)e^{-6Dt} \quad [3]$$

$$D = k_b T / 8\pi b^3 n, \quad [4]$$

where b is the hydrodynamic (Stokes) radius of the sphere, n is the viscosity of the solvent in poise, k_b is Boltzmann's constant, and T is the absolute temperature. The intrinsic anisotropy at zero time, $r(0)$, is determined by the electronic properties of the chromophore; theoretical calculations for a dipole moment yield $r(0) = 0.40$ (10).

For a rigid rod or cylinder, Favro (11) and Tao (12) have shown that the anisotropy decays as a sum of three exponentials:

$$r(t) = (2/5) \times \left\{ \left(\frac{3}{4} \sin^4 \theta \right) e^{-(2D_{\perp} + 4D_{\parallel})t} + (3 \cos^2 \theta \sin^2 \theta) e^{-(5D_{\perp} + D_{\parallel})t} + [(3 \cos^2 \theta - 1)/2]^2 e^{-6D_{\perp}t} \right\}, \quad [5]$$

where θ is the polar angle between the dipole moment of the intercalated dye and the long axis of the cylinder and D_{\parallel} and D_{\perp} are the diffusion constants for rotations about the long axis of the cylinder (spinning) and around the two short axes (end-over-end tumbling), respectively.

For rigid rods, the expressions for the diffusion coefficients D_{\parallel} (13) and D_{\perp} (14) are

$$D_{\parallel} = k_b T / 8\pi n b^2 L \quad [6]$$

and

$$D_{\perp} = 3k_b T / 8\pi n L^3 \times (\ln(2L/b) - 1.57 + \{[(1/\ln(2L/b)) - 0.28]^2\}) \quad [7]$$

where $2L$ and $2b$ refer to the length and diameter of the rod.

The initial anisotropy at $t = 0$ should be 0.40 for a dipole moment. Decrease of this value from the initial value can be due to several causes. (i) Multiple excitations of a molecule during the laser pulse can change the initial dipole moment excitation distribution from the $\cos^2 \theta$ expected for a dipole. (ii) The dipole moment of the monitored state is at an angle δ from the excitation dipole. (iii) The excitation or monitored states (or both) are not simple dipole moments.

We have carried out intensity-dependence variations that show that *i* is not the cause of our $r(0)$ of 0.25 for methylene blue and 0.16 for the intercalated dye. Only single crystal work will allow distinguishing between *ii* and *iii*, which we have not done. In the absence of this knowledge, our approach has been to simply renormalize the theoretical models to our initial anisotropy. This procedure is correct only if the initial anisotropy is low due to a departure from a $\cos^2 \theta$ distribution of excited dipoles. If the absorption and emission dipoles are at an angle δ with respect to each other, the amplitudes of the anisotropy components are affected (refs. 10, 15) and simple renormalization is not correct. However, since we monitor singlet depletion, the absorption moments are by definition the same as what could be called the emission moments and so Tao's formula can be used here with renormalization. The procedure seems valid: the short fragments, which are expected to tumble rigidly, do have the expected corrected long time-component amplitude.

Eqs. 5, 6, and 7, while applicable to rigid rods, can be considered no more than a first-order approximation to the expected anisotropy decay of DNA. In solution, the B-form helix is not a completely rigid molecule. A measure of the stiffness of the helix is given by its persistence length, which is defined as the average projection of the molecule on an axis parallel to the helix at one end (16). Barkley and Zimm (17) and, independently, Allison and Schurr (18) have derived expressions for the anisotropy decay that attempt to account for the bending and twisting motions of DNA. The theory of Barkley and Zimm is of more interest to us, however, because it attempts to take bending motions into account. Barkley and Zimm assume a uniformly elastic rod and make small-angle approximations to separate the torsional and bending decay functions and solve for the normal modes of motion.

$$r(t) = [1/3(2 - \sin^2 \theta) + (3 \sin^2 \theta - 2)e^{-\Delta(t)}] \times \{0.4(3 \sin^2 \theta - 2)^2 e^{-\Delta(t)} + \sin^4 \theta [0.75e^{-\Gamma(t)} + 0.45e^{-\Gamma(t) + \Delta(t)}] + 4.8 \sin^2 \theta \cos^2 \theta e^{[-\Delta(t) + \Gamma(t)/4]}\}, \quad [8]$$

where $\Gamma(t)$ and $\Delta(t)$ are, respectively, the bending and twisting decay functions for the normal deformation modes of a flexible rod.

Since the Barkley-Zimm theory assumes that only small displacements occur, its applicability is limited to the earliest times of the anisotropy decay and is expected to fail at long times when the large-angle tumbling components of the decay become important. In Fig. 1, we present a schematic of the general time

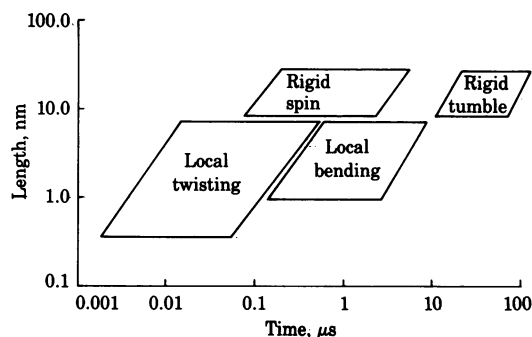


FIG. 1. Time and length ranges for which DNA rotational motion is important in different theories. We assume a fragment of one persistence length (60 nm) and a torsional modulus of 1.7×10^{-19} erg-cm. The regions marked "local twisting" and "local bending" come from the Barkley-Zimm theory and the "rigid spin" and "tumble" regions come from the theory of Tao and the diffusion constants of Broersma.

and length ranges for a DNA fragment of one persistence length (180 bp) to indicate the areas where the present theory has some validity.

RESULTS

We have characterized in detail the binding of methylene blue to DNA. As summarized in Table 1, methylene blue binds tightly to DNA under standard conditions; $K = 6 \times 10^4 \text{ M}^{-1}$ as measured by phase partitioning (19) and fluorescence techniques (20). We used electric dichroism techniques (22) to measure the orientation of the methylene blue absorption transition moment relative to the long helix axis (71.5°) and the DNA length increase that occurs upon binding (2.9 Å per dye molecule).

In general, the properties measured for the methylene blue-DNA complex are similar to those of other intercalating

Table 1. Properties of methylene blue and binding to calf thymus DNA

Property	Methylene blue	
	Bound	Free
A_{max} ,* nm	675	665
Molar extinction coefficient	36×10^3	44×10^3
Emission maximum,† nm	686	683
Relative fluorescence change on binding to DNA‡	0.20	1
Triplet lifetime in deaerated buffer, μs	73	28
Initial anisotropy in standard buffer/98% glycerol	0.16	0.25
K_a ,§ M^{-1}	6×10^4	
Orientation of singlet-singlet transition moment, deg	71.5	
DNA length increase per methylene blue molecule bound,¶ Å	2.9	

Except where noted otherwise, properties of bound methylene blue were measured at 5°C in standard buffer in the presence of excess calf thymus DNA.

* Measured on a Cary 14 spectrophotometer.

† Measured on a Perkin-Elmer spectrofluorimeter.

‡ Measured with excitation at 665 nm and monitoring at 683 nm.

§ Measured by phase partitioning against 30% pentane/70% pentanol (19) and by fluorescence titration (20).

¶ Measured with respect to the long helix axis in 5 mM Tris-HCl/0.5 mM Na_2EDTA , pH 7.5, by transient electric dichroism experiments (21) using 157 ± 15 -bp-long DNA at 5°C .

|| Measured by transient electric dichroism techniques (21).

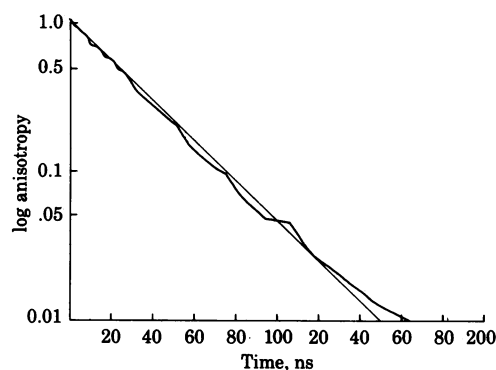


FIG. 2. Anisotropy decay of methylene blue in 61.5% sucrose/ H_2O at 5°C plotted as a semilog graph. Data are normalized to 1.0; the initial value was 0.12 as opposed to the maximum value of 0.25 observed in 95% glycerol. This loss in initial anisotropy is most likely due to rotation during the excitation pulse. Note the absence of distortion at short times even with the inclusion of the 15-ns laser pulse. The slope of the least-squares fit to the data gives a decay time of 33 ns.

dyes (22). Therefore, we conclude that methylene blue binds to DNA by intercalating into the helix.

As shown in Table 1 (and Fig. 3), the initial anisotropy $r(0)$ of methylene blue intercalated into DNA is 0.16, as determined from the initial value of methylene blue intercalated in 600-bp fragments in 80% glycerol/water. The 0.16 initial anisotropy value is smaller than the value expected for a simple linear dipole. However, such reduced initial anisotropy values are often seen in triplet measurements (23). The initial anisotropy measured for free methylene blue in a high viscosity medium (98% glycerol) is 0.25.

Fig. 2 shows the anisotropy decay of methylene blue in 61.5% (wt/wt) sucrose/ H_2O at 5°C . The anisotropy decays as a single exponential with time constant 33 ns. This value yields from Eq. 3 an apparent Stokes radius of 0.36 nm for the methylene blue molecule, which is consistent with its molecular dimensions ($0.5 \times 0.10 \times 0.30$ nm), indicating that our apparatus can resolve a 33-ns decay time accurately.

Fig. 3 shows the anisotropy decays of several DNA fragments plotted as the logarithm of the anisotropy vs. the logarithm of the time scale. Four decades in time are covered; however, the data at <10 ns may be distorted by convolution with the laser pulse.

The results of three-exponential fits to our anisotropy decay data as well as the amplitudes and time constants expected for

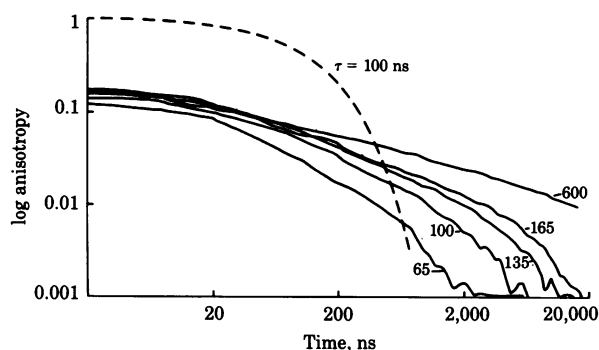


FIG. 3. Full log-log plot of the anisotropy decay of methylene blue intercalated into defined-length fragments of calf thymus DNA. Data are smoothed by a moving logarithmic average. An exponential with a lifetime (τ) of 100 ns and an amplitude of 1.0 (---) is shown so that the reader can compare the curves with a familiar function. All lengths given are ± 15 bp. The 65-bp fragment shows a reduced initial amplitude due to molecular motion during the laser pulse.

Table 2. Comparison between fits to data and rigid rod simulations

Fragment	Computer fit			Graphic fit (long)	Rigid-rod simulation		
	Long	Medium	Short		Long	Medium	Short
600 bp							
τ , μs	38	3.2	0.34	25	162	1.6	0.39
Amplitude	0.013	0.019	0.066	0.017	0.018	0.04	0.09
165 bp							
τ , μs	4.2	0.47	0.069	5.1	5.2	0.43	0.11
Amplitude	0.021	0.030	0.06	0.017	0.018	0.04	0.09
135 bp							
τ , μs	2.9	0.27	0.055	3.8	3.2	0.34	0.09
Amplitude	0.021	0.04	0.07	0.015	0.018	0.04	0.09
100 bp							
τ , μs	1.3	0.14	0.064	1.9	1.5	0.25	0.07
Amplitude	0.024	0.03	0.07	0.016	0.018	0.04	0.09
65 bp							
τ , μs	0.34	0.80	0.026	0.38	0.58	0.14	0.05
Amplitude	0.026	0.03	0.07	0.02	0.018	0.04	0.09

Time constants (τ) and amplitudes are given for three-exponential fits and the values predicted from Eq. 5. Computer fits were made to a triplet exponential with no baseline. Except for the 65-bp fragment, all data were fit to files stored at a 20 ns per point sample interval. Anisotropy data were analyzed by a three-exponential fitting program based on a least-squares steepest-descent algorithm (24). Except for the last, slowest component of the decay, the data were not expected to fit a multiexponential function, and therefore the derived fits should be treated as empirical values that characterize the data.

rigid-rod rotation with normalization due to initial depolarization (calculated from Eqs. 5–8) are given in Table 2.

Simulated anisotropy decay curves were computed by using both the rigid-rod and the Barkley–Zimm theories. Both simulations used a value of 0.33 nm per bp (25) to compute fragment lengths and a hydrated helix diameter of 2.6 nm. In the Barkley–Zimm calculations, we used a value of 1.75×10^{-19} erg·cm (1 erg = 0.1 μJ) for the torsional rigidity, C , of the DNA. If we assume that the DNA can be viewed as a uniformly elastic rod, as do Barkley and Zimm, then the expression derived by Landau and Lifschitz for the persistence length (26) and the measured persistence length of DNA at 5°C and 0.1 M NaCl (66 ± 6 nm) (27) yield this value. For simplicity, we show in Fig. 4B data and simulations for the 165-bp fragments only; however, the conclusions discussed also apply to all other fragments shorter than one persistence length.

We have two classes of DNA fragments in our work: those with contour lengths less than one persistence length (165-, 135-, 100-, and 65-bp fragments) and those longer than one persistence length (the 600-bp fragment). We will look first at the fragments of less than one persistence length.

For short fragments, the longest component of anisotropy decay monitors end-over-end tumbling of the helix. As shown in Fig. 4A and Table 2, the amplitude and decay time measured for that long component are in good agreement with the value predicted for a rigid-rod-like helix. This suggests that, for DNA fragments shorter than one persistence length, the long helix axis is rigid. DNA bending motions must not occur at times commensurate with rigid end-over-end tumbling since such local bending would reduce both the amplitude and decay time of the longest components of anisotropy decay. The Barkley–Zimm theory deviates substantially here, as expected, because they assumed small displacements for the DNA motions, which obviously cannot hold as the anisotropy goes to zero.

For a rigid rod, we expect two faster components due to rigid spinning of the rods around the major axis. However, our data show a faster anisotropy decay than that predicted by the rigid rod. We take this to mean that there are local twisting modes of substantial amplitude that invalidate the rigid-rod model at times $< 1 \mu\text{s}$. We expect that the Barkley–Zimm model should

afford a better fit to the data in short-time regime. As shown in Fig. 4B, our simulations indicate that this model predicts too fast a decay. Thus, while we do see evidence for local twisting,

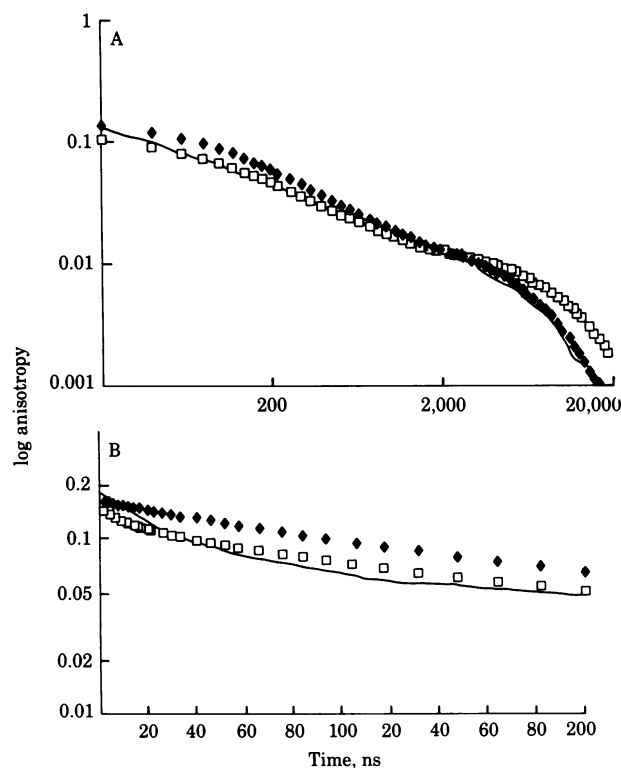


FIG. 4. Anisotropy decay of a 165-bp-long DNA fragment (—) compared with Barkley–Zimm (\square) and rigid-rod (\blacklozenge) simulations for fragments of the same length. (A) Simulations were done assuming a DNA radius of 1.3 nm, a rise of 0.33 nm per base pair, $T = 5^\circ\text{C}$ (278K), viscosity = 0.015 poise, and $C = 1.75 \times 10^{-19}$ erg·cm (for the Barkley–Zimm simulation). (B) Data from A were replotted on a semilog graph with an expanded time scale. The 165-bp fragments do not have as much short-time motion as Barkley–Zimm simulation predicts nor do the data agree with the rigid-rod simulations.

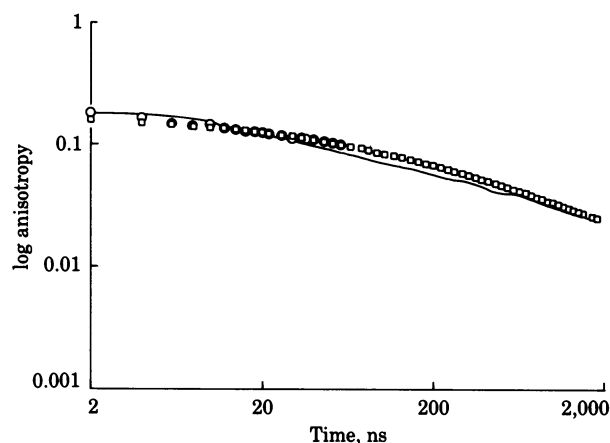


FIG. 5. Comparison of anisotropy decay of a 600-bp DNA fragment (—) with the Barkley-Zimm prediction (\square) and fluorescence anisotropy data (\circ ; ref. 5). Data are plotted on a log-log scale for the first $2 \mu\text{s}$ of decay. Ref. 5 data and Barkley-Zimm predictions are normalized to match the initial anisotropy of 0.16.

even in short fragments, Barkley and Zimm seem to overestimate the time course of this process.

The 600-bp data are fit quite well by the Barkley-Zimm model in the 10-ns to 2- μs time range. This indicates to us that the failure of this model in short fragments is due to the assumption that the dye is the middle of the DNA—i.e., the neglect of end effects. Our data do seem to indicate that, for fragments for which the contour length is sufficient to ignore end effects and the total anisotropy decay is small enough to allow the small-angle approximation, the Barkley-Zimm model gives a good fit. As expected, both Barkley-Zimm and rigid rod are of no use in predicting the long time component of the 600 bp decay.

Fig. 5 shows both the triplet-state anisotropy decay and the fluorescence anisotropy decay of ethidium bromide bound to long DNA fragments (data from ref. 5); after normalization to the same initial anisotropy (to account for electronic differences in the two dyes), fluorescence and triplet-state anisotropy decay curves are nearly identical. Therefore, (even though the time range accessible to fluorescence measurements is limited) over the short time range in which both fluorescence and triplet-state anisotropy can be measured, the two techniques appear to monitor the same molecular motions.

CONCLUSIONS

We have used triplet anisotropy decay to measure the flexibility of DNA. From this work, we conclude that no current theory can describe quantitatively the motion of a DNA helix in solution. However, based on our measurements, two general conclusions can be drawn concerning the dynamics of DNA structure. For DNA fragments shorter than one persistence length (≈ 200 bp), the long axis of the helix appears to be very rigid.

Anisotropy decay of very long helices diverges from that rigid behavior, indicating that (as expected) long DNA helices experience segmental motion. Based on the rigidity of the long helix axis, we conclude that the fast initial decay of methylene blue anisotropy is due to torsional motions of the DNA helix. The time constant for these motions appears to be 50 ns.

We thank Tom Jovin, who initiated these experiments and has contributed valuable advice; Don Crothers for use of the field jump facilities; Nani Dattagupta for help with field jump measurements; Chris Raymond for creation of the fitting code and plotting routines; and Shirley Chan for support and advice. We also thank Mickey Schurr and Attila Szabo for sharing prepublication work and Leonard Lerman for constructive criticism. This work was funded by National Institutes of Health Grant GM 2904701 and American Cancer Society Grant NP352.

- Klevan, L., Armitage, I. M. & Crothers, D. M. (1979) *Nucleic Acids Res.* **6**, 1607–1616.
- Hogan, M. E. & Jardetzky, O. (1979) *Proc. Natl. Acad. Sci. USA* **76**, 6341–6345.
- Bolton, P. H. & James, T. L. (1980) *J. Am. Chem. Soc.* **102**, 23–32.
- Hogan, M. E. & Jardetzky, O. (1980) *Biochemistry* **19**, 2079–2085.
- Millar, D. P., Robbins, R. J. & Zewail, A. H. (1980) *Proc. Natl. Acad. Sci. USA* **77**, 5593–5597.
- Wahl, P., Paoletti, J. & LePecq, J.-B. (1970) *Proc. Natl. Acad. Sci. USA* **65**, 417–421.
- Thomas, J. C., Allison, S. A., Appellof, C. J. & Schurr, J. M. (1980) *Biophys. Chem.* **12**, 177–188.
- Robinson, B. H., Lerman, L. S., Beth, A. H., Frisch, H. L., Dalton, L. R. & Auer, C. (1980) *J. Mol. Biol.* **139**, 19–44.
- Austin, R. H., Chan, S. S. & Jovin, T. M. (1979) *Proc. Natl. Acad. Sci. USA* **76**, 5650–5654.
- Belford, G. G., Belford, R. L. & Weber, G. (1972) *Proc. Natl. Acad. Sci. USA* **69**, 1392–1393.
- Favro, L. D. (1960) *Phys. Rev.* **119**, 53–62.
- Tao, T. (1969) *Biopolymers* **8**, 609–632.
- Lamb, H. (1945) *Hydrodynamics* (Dover, New York).
- Broersma, S. (1960) *J. Chem. Phys.* **32**, 1626–1631.
- Lipari, G. & Szabo, A. (1980) *Biophys. J.* **30**, 489–506.
- Cantor, C. & Schimmel, P. R. (1980) *Biophysical Chemistry Part III: The Behavior of Biological Macromolecules* (Freeman, San Francisco), p. 1012.
- Barkley, M. D. & Zimm, B. H. (1979) *J. Chem. Phys.* **79**, 2991–3007.
- Allison, S. A. & Schurr, J. M. (1979) *Chem. Phys.* **41**, 35–59.
- Waring, M. J., Wakelin, L. P. G. & Lee, L. S. (1975) *Biochim. Biophys. Acta* **407**, 200–212.
- LePecq, J.-B. & Paoletti, C. (1967) *J. Mol. Biol.* **27**, 87–106.
- Hogan, M., Dattagupta, N. & Crothers, D. M. (1978) *Proc. Natl. Acad. Sci. USA* **75**, 195–199.
- Hogan, M., Dattagupta, N. & Crothers, D. M. (1979) *Biochemistry* **18**, 280–288.
- Jovin, T. M., Bartholdi, M., Vaz, W. L. C. & Austin, R. H. (1981) *Ann. N.Y. Acad. Sci.* **366**, 176–196.
- Bevington, P. R. (1969) *Data Reduction and Error Analysis for the Physical Sciences* (McGraw-Hill, New York).
- Wing, R., Drew, H., Takano, T., Broka, C., Tanaka, S., Itakara, D. & Dickerson, R. E. (1980) *Nature (London)* **287**, 755–758.
- Landau, L. D. & Lifschitz, E. M. (1958) *Statistical Physics* (Addison-Wesley, Reading).
- Jolly, D. & Eisenberg, H. (1976) *Biopolymers* **15**, 61–95.